

NONTRIVIAL EMBEDDINGS OF POLYGONAL INTERVALS AND UNKNOTS IN 3-SPACE

JASON CANTARELLA and HEATHER JOHNSTON

Mathematics Department
University of Pennsylvania
Philadelphia, PA 19104
cantarel@math.upenn.edu

Mathematics Department
Rutgers University
New Brunswick, NJ 08903
hjohnst@math.rutgers.edu

ABSTRACT

We consider embedding classes of polygonal intervals and circles with fixed edge lengths. We classify all embeddings of polygonal lines of five segments, finding that this space has three connected components for suitable edge lengths. We then construct a class of “stuck” unknotted hexagons, which cannot be deformed to the standard unknotted hexagon. The edge lengths of our examples are not equal.

Keywords: polygonal knots, space polygons, geometric knots

1. Introduction

In this paper, we consider the following situation. A chain of n line segments with lengths l_1, \dots, l_n embeds in \mathbf{R}^3 . We study the space of such embeddings, denoted $\text{Ch}_n(l_1, \dots, l_n)$. If the chain closes, it forms a space polygon of side lengths (l_1, \dots, l_n) . The space of such polygons is denoted $\text{Pol}_n(l_1, \dots, l_n)$.

The study of embedding classes of such objects constitutes a kind of PL knot theory, of particular relevance in computer models in knot theory, as well as in algebraic geometry. These questions were examined by Randell in 1988 [1], and have later been studied by Millett [2] and many other authors. Energies for polygonal knots have been studied quite extensively (see, for instance, Simon [3] or Diao, et. al. [4]), and the topic of random knotting of polygonal knots has been examined by many authors (see Sumners and Whittington [5]). Until now, the following question has been open: Are the connected components of Pol_n simply knot types, or do there exist distinct embeddings of the same knot?

We start by answering this question for all $\text{Ch}_5(l_1, \dots, l_5)$. Of course, all chains have the same topology, so if Ch_n is disconnected, the geometry must be responsible. If l_1 and l_5 are greater than $l_2 + l_3 + l_4$, there are three distinct embeddings of five sticks. Otherwise, there is only one class of embeddings.

We next consider the case of space polygons. Millett and Orellana proved in 1994 that the class of unknots in $\text{Pol}_6(1, 1, 1, 1, 1, 1)$ is connected [2]. Recently, Calvo has shown that if we consider orientation, there are distinct embeddings of left and right-handed trefoils in $\text{Pol}_6(1, 1, 1, 1, 1, 1)$ [6]. Our main result is that there exist

“stuck” unknots which cannot be deformed to convex polygons, for suitable choices of edge length, in Pol_n for all $n \geq 6$.

The picture below shows (left) a stuck unknot in Pol_6 , and (right) a stuck chain in Ch_5 .

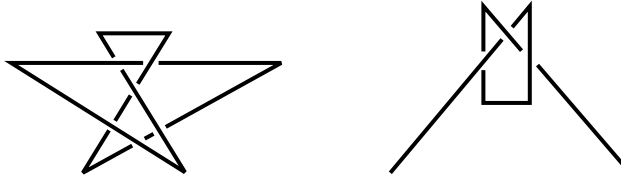


Figure 1: Some examples.

2. Chains

For the duration of this section, we will consider only chains. Our method is to study the projection $\text{Ch}_{n+1} \xrightarrow{p} \text{Ch}_n$ given by deleting the last segment of each chain.

This map does *not* have the path lifting property. To see this, realize that the ability to lift a path from the “base” Ch_n would imply that any deformation of the first n segments of the chain could be performed with the last segment present. The picture below (left) shows a situation where this is not possible. For simplicity, only the relevant segments appear. The last segment is dotted. The arrows show a deformation of the first n segments which will be stopped by the last segment.

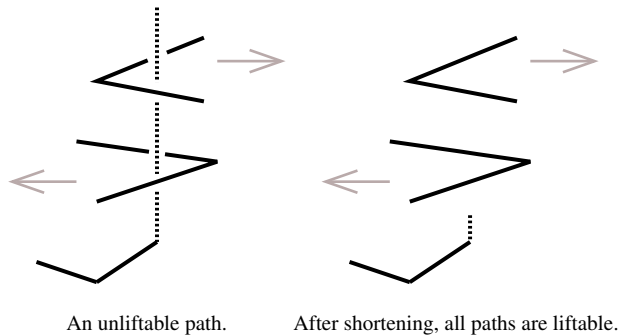


Figure 2: Lack of path-lifting property.

It is interesting to contrast this situation with the case where the number of segments is fixed, but their lengths are allowed to vary. We denote this configuration space by Ch'_n . In this case, the projection $\text{Ch}'_{n+1} \xrightarrow{p} \text{Ch}'_n$ has the path lifting property.

To prove it, we make the following observation. For *any* path $\alpha : I \rightarrow \text{Ch}'_n$, there is some length of time $\epsilon > 0$ before $\alpha(t)$ intersects the last segment. To lift α , use this time to shrink the last segment until it does not interfere with the first n segments, as above (right). Then use another ϵ of time to rotate the last segment until it is colinear with the n th segment. The last segment is kept in this position for the remainder of the path.

We may now prove our first lemma.

Lemma 1. *If the lengths of the segments are allowed to vary, each point inverse $p^{-1}(x_0)$ of the projection $\text{Ch}'_{n+1} \xrightarrow{p} \text{Ch}'_n$ is connected. Thus, each Ch'_n is connected.*

Proof. Consider the effect of shrinking the last segment of each configuration in Ch'_{n+1} . This shrinking is a deformation retraction of each point inverse $p^{-1}(x_0)$ of the projection $\text{Ch}'_{n+1} \xrightarrow{p} \text{Ch}'_n$ onto the space of embedded configurations of a line segment attached at one end to another line. By considering the sphere placed at the vertex between the n th segment and the $(n+1)$ st segment, we can see that this configuration space is clearly $S^2 - \{pt\}$, as shown below. Note that this implies each point inverse is connected.

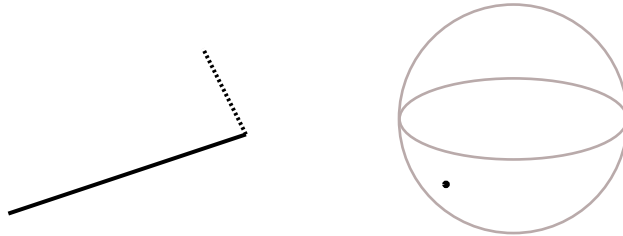


Figure 3: The configuration space of the dotted line is $S^2 - \{pt\}$.

The dot marks the spherical image of the n th segment.

Note that this implies that the Ch'_n are all connected. Since Ch'_1 is obviously connected, the result follows inductively using the path lifting property and the connectedness of point inverses. \square

This lemma tells us where new information enters the picture. We must pay attention to the relative lengths of the segments, if we are to find a more interesting entanglement theory!

We now return to the case where the lengths of the segments are fixed. Let us first introduce a bit of terminology. The basepoint of each $\text{Ch}_n(l_1, \dots, l_n)$, denoted by e , will be the configuration where all segment angles are equal to π — the straight line.

We now prove our next lemma.

Lemma 2. *For $n < 5$, $\text{Ch}_n(l_1, \dots, l_n)$ is connected for all l_i .*

Proof. Again we proceed by induction. We refer to $\text{Ch}_n(l_1, \dots, l_n)$ as Ch_n for the duration of the proof. Ch_1 is connected. Consider the general case $\text{Ch}_{n+1} \xrightarrow{p} \text{Ch}_n$. As we saw in the proof of Lemma 1, the inverse image $p^{-1}(x_0)$ is the configuration space of a line segment, attached at one end to another line, which cannot intersect a certain number of other line segments elsewhere in space. It is easy to see that the effect of these constraints is to remove a certain number of segments of great circles, together with a point, from the sphere shown in the proof of Lemma 1.

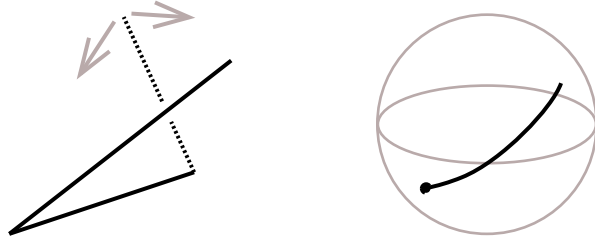


Figure 4: Adding segments removes great-circle arcs from S^2 .

We can make the following observations about the situation:

- There are no more than $n - 1$ segments.
- Each segment has (spherical) length $< \pi$.
- The length of each segment, and whether the spherical segments are connected, depends on the length of the last line segment — for very long line segments, the chain of spherical segments is always connected.

Items one and two now tell us that fiber and base are connected for $n \leq 4$. After all, it requires three great-circle segments of length $< \pi$ to enclose an area on S^2 .

If each inverse image $p^{-1}(x_0)$ is connected, and Ch_n is connected, then we will show that Ch_{n+1} is connected by constructing a path from any point x in Ch_{n+1} to the basepoint of Ch_{n+1} .

To do this, assume that $p(x) = x_0$, and consider the the point in the inverse image $p^{-1}(x_0)$ antipodal to the dot marking the image of the n th segment. Since $p^{-1}(x_0)$ is connected, the $(n+1)$ st segment can (generically) be moved to this point. We have then straightened out the last corner in our configuration, reducing it to a configuration in Ch_n . Since Ch_n is connected, we have a path from here to the basepoint. \square

To investigate the embedding theory of Ch_5 , we must investigate the structure of the point inverses $p^{-1}(x)$ under the projection $\text{Ch}_5 \xrightarrow{p} \text{Ch}_4$. To do this, we consider the possible configurations of three great-circle segments of length $< \pi$ on S^2 . For the duration of the discussion, we'll omit the sphere in our illustrations, and the words “great-circle” when we refer to the segments on the sphere.

Since each configuration in Ch_4 comes with an orientation, each collection of spherical segments comes with an orientation, as well. This means that if the segments are connected, there are only three possible cases. Of course, the segments are not always connected— if the last segment is short, its motion will not be obstructed by the portions of other segments which are too far away.

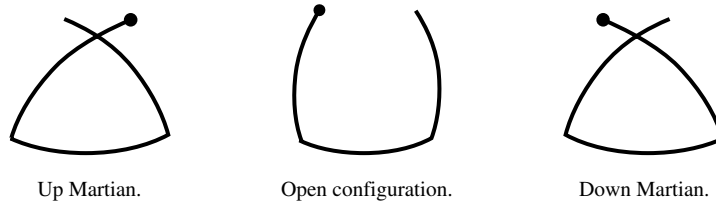


Figure 5: Up and down martians.

In the pictures in this section, the point on the sphere denoted \bullet is the spherical image of the fourth segment of the given configuration, while the spherical image of the last segment will be denoted y . The left and right configurations are referred to as *up* and *down martians*. The words up and down denote position of the right-hand rule orientation given by the numerical ordering of sticks in the loop compared to the standard orientation on S^2 .

In all these cases, given some configuration $x \in \text{Ch}_5$ with $p(x) = x_0$, we'll refer to the configuration of the three segments as $C(x_0)$.

We state our main result immediately.

Theorem 1. *The space $\text{Ch}_5(l_1, \dots, l_5)$ has three connected components if we have $l_1 \geq l_2 + l_3 + l_4$ and $l_5 \geq l_2 + l_3 + l_4$, and one connected component otherwise. One of these contains the basepoint e , while the others contain the “stuck” configurations k and \bar{k} pictured below.*

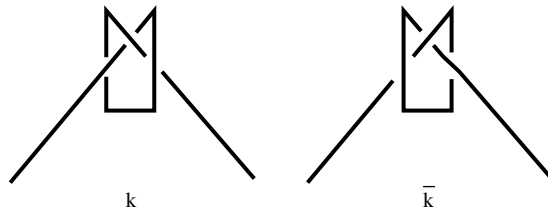


Figure 6: Two nontrivial embeddings in Ch_5 .

Proof. We start by giving an outline of the proof. We will then prove the lemmas mentioned below. First, since Ch_4 is always connected by Lemma 2 above, we observe that if any corner of a configuration in Ch_5 can be straightened, that configuration can be deformed to e .

By Lemma 3, if $C(x_0)$ is a martian, the point antipodal to \bullet is outside the martian. This will imply that if $C(x_0)$ is not a martian, or if y is outside $C(x_0)$, the configuration x may be deformed to e . By reversing the orientation of x and repeating these arguments, we get corresponding statements about the position y' of the *first* segment relative to the configuration $C(x'_0)$ of the *last* four segments. Thus the only remaining case is where y and y' are inside the corresponding martians $C(x_0)$ and $C(x'_0)$.

In this case, by Lemma 4, there is no obstacle to deforming x into a “stretched” configuration (see the proof). From this, we can see that if $l_5 < l_2 + l_3 + l_4$, we can continue to stretch the configuration x until a corner of the martian $C(x_0)$ disappears. Then we can move the point y outside the martian $C(x_0)$, straighten the last corner of x , and thus deform x to configuration e . By the same argument, if $l_1 < l_2 + l_3 + l_4$, we can again deform x to configuration e .

We are now left with the case where both y and y' are in the corresponding martians $C(x_0)$ and $C(x'_0)$ and $l_1 \geq l_2 + l_3 + l_4$, while $l_5 \geq l_2 + l_3 + l_4$. In this case, Lemma 5 proves that $C(x_0)$ and $C(x'_0)$ remain connected after any isotopy of the polygon.

We next show in Lemma 6 that $C(x_0)$ and $C(x'_0)$ remain martians under any isotopy. It follows that there is no path from x to e .

Further, there is no deformation of x which changes the orientation of $C(x_0)$ or $C(x'_0)$. *A priori*, it would appear that there are four embeddings, since each martian is either up or down. In fact, only two combinations are possible: up-up and down-down. We prove this in our last lemma. Thus there is no path from k to \bar{k} , or from either to e . This will complete the proof.

Lemma 3. *The point antipodal to \bullet is outside the martian $C(x_0)$.*

Proof. Define the side containing the point \bullet to be the outside of a martian. This definition is consistent (if necessary, perturb the martian), but does not always agree with the standard definition derived from the orientation. The picture below holds. Since segment CA intersects AB at A , it cannot intersect the dotted line segment. \square

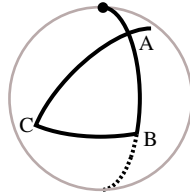
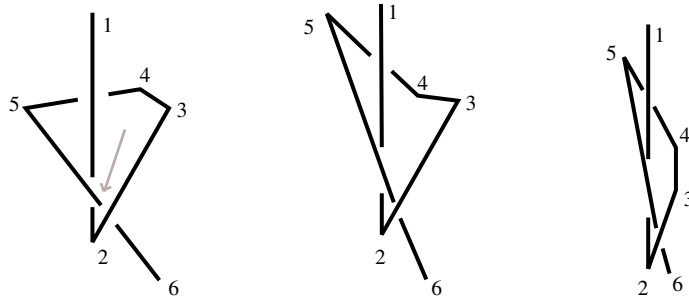


Figure 7: The point antipodal to \bullet is outside the martian.

Lemma 4. *If y and y' are in the martians $C(x_0)$ and $C(x'_0)$, given any $\epsilon > 0$ we can deform x until the angles at vertices 3 and 4 of x are within ϵ of π .*

Proof. To make things easier, we make a few assumptions for the proof. First, we assume that vertices 1 and 2 lie along the z -axis. Next, we assume that vertex 3 lies in the y - z plane with positive y coordinate. Last, we assume that vertex 4 has negative x coordinate.

These choices amount to a rigid motion of the entire chain, and a choice of orientation of the first martian. We have, generically, the diagram below. Further, we may assume that the first edge remains fixed, and the second remains in the y - z plane.



Slide 6 close to the corner. 5 must have positive x coordinate. We can still stretch!

Figure 8: Constraints on the motion of edges 2, 3 and 4.

We now realize that we are free to take all motions of edges 2, 3 and 4 which keep one end of 2 at the origin, avoid the z -axis, and keep vertex 4 behind the y - z plane. These constraints present no obstruction to stretching the joints as above. \square

Lemma 5. *If $l_1 \geq l_2 + l_3 + l_4$ then x cannot be deformed to disconnect $C(x_0)$.*

Proof. Consider the sphere centered at the second vertex of x , with radius l_1 . The martian $C(x_0)$ is the radial projection of the portion of x inside the sphere onto the sphere. Since x is connected, the projection is disconnected only if x leaves the sphere and then enters it again.

However, our constraint on the lengths of the segments implies that the only vertex of x which can be outside the sphere is the last vertex. This means that the portion of x outside the sphere is a line segment, and so x cannot reenter the sphere. \square

Lemma 6. *Suppose x is such that $C(x_0)$ is a martian, and x obeys our length constraints. If there is an isotopy of x which opens $C(x_0)$, then y' must be outside $C(x'_0)$.*

Proof. We start by thinking about isotopies which open the martian.

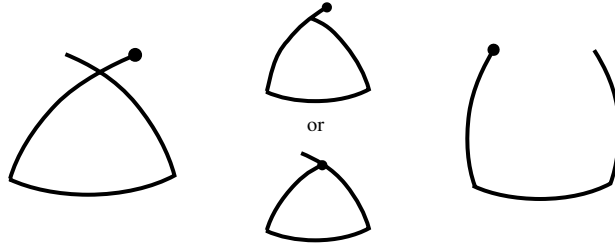


Figure 9: To open the martian we must pass through a middle configuration.

Clearly, this leaves us with two cases. In the first, we have the situation below.

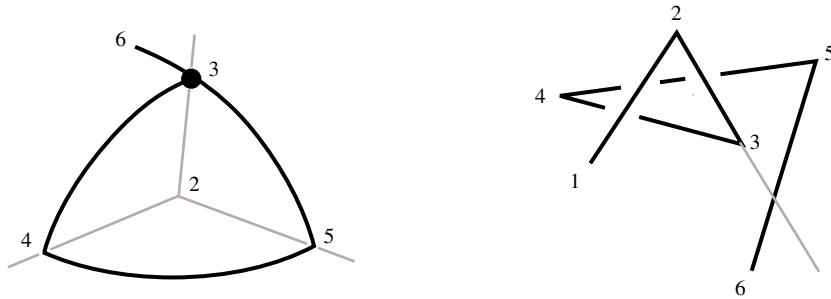


Figure 10: The first case.

From the picture, we see that edge 5 must cross the line from vertex 2 to vertex 3. Thus, from the point of view of 5, the image of point 6 (that is, y'), is on the arc of a great circle formed by extending a side of the martian $C(x'_0)$. In particular, y' is outside $C(x'_0)$.

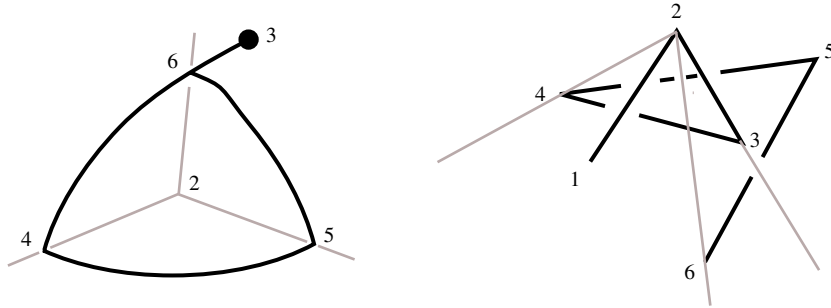


Figure 11: The second case.

The point 6 must lie in the sector of a plane defined by points 2, 3, and 4 shown by the gray lines above. However, our length constraints imply that 6 is outside the triangle formed by 2, 3 and 4. Again, from the point of view of vertex 5, y' is outside $C(x'_0)$. \square

Lemma 7. *There are exactly two types of “stuck” configurations in which both points y and y' are inside their respective martians $C(x_0)$ and $C(x'_0)$: the configurations k and \bar{k} as given above.*

Proof. Each martian is oriented up or down. We must prove that the orientations agree. Let’s consider the choices we made in the proof of Lemma 4, and refer back to figures from that argument.

If we chose the x coordinate of vertex 4 to be negative, we found that the x coordinate of 5 had to be positive. Thus, the martian formed by edges 1, 2 and 3 was oriented *up*.

On the other hand, we also found that edges 3, 4, and 5 encircled the z -axis counterclockwise. Since vertex 6 must be above all these by our length constraints, the martian formed by edges 3, 4 and 5 must also be oriented *up*. If we chose the x coordinate of vertex 4 to be positive, all the orientations would be reversed, and the orientations of both martians would be *down*. \square

Given that all other configurations are equivalent to the trivial configuration, this lemma completes our classification of the embeddings of five-segment open polygons. \square

3. Stuck Unknots: An Example

We now study the set of closed polygons, $\text{Pol}_n(l_1, l_2, \dots, l_n)$. This section is devoted to proving that stuck unknots exist. In particular, we will prove that in every Pol_n , for $n > 5$, there exist topological unknots which cannot be deformed (while preserving edge-length) to the standard planar unknot. An easy corollary will be that as n becomes large, the number of different classes of unknots grows without bound!

This stands in stark contrast to the case for equilateral polygons— as n increases, our theory does *not* converge to the continuous case. Thus, our results depend essentially on the fact that the edges have different lengths. We do not see how to construct corresponding results in the equilateral case, and we suspect that it is impossible.

Here is an example in Pol_6 , reproduced from the first page of the paper.

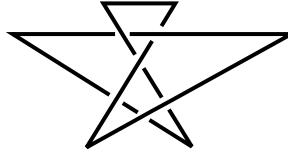


Figure 12: Our example in Pol_6 .

The idea of our proof is to use the geometry of the situation to construct a correspondance between polygonal knots and strings. We will then prove that the strings corresponding to our examples are nontrivial. Since this last result takes place in the continuous category, we will be able to add as many joints as we like without changing the embedding class of the string.

Theorem 2. *For suitable choices of edge-length, there is more than one isotopy class of embeddings of the unknot in $\text{Pol}_6(l_1, \dots, l_6)$.*

Proof. The proof proceeds by constructing an embedding of the unknot which is *not* isotopic to the standard embedding of the unknot as a convex polygon. The desired embedding is given by the coordinates in the table below.

Table 1: Coordinates for a stuck unknot.

Vertex	1	2	3	4	5	6
Coordinates	(0,0,-50)	(0,0,50)	(20,-5,-10)	(-2,2,2)	(-2,-2,-2)	(20,5,10)

We recall the definition of a *string*, from classical knot theory. A string is a collection of arcs or strands connecting two parallel planes in \mathbf{R}^3 . A string isotopy consists of a motion of the strands and their endpoints which keeps the endpoints of each strand in the specified plane. Note that any braid is a trivial string, because it may be “unraveled” by an allowable motion of the endpoints. In contrast to the idea of a braid, the strands in a string are *not* required to always run in the same direction.

Here is an example of a two-strand string which deforms to a trivial two-strand string, together with the corresponding string isotopy.

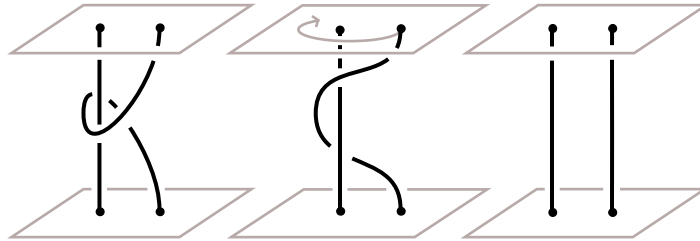


Figure 13: An example of a string-isotopy. Notice that the endpoints can move.

Without loss of generality, fix the first edge for the remainder of the proof. Now, observe that in our given configuration, if we take two planes perpendicular to the first edge, at vertices 1 and 2 of the polygon, and replace edges 2 and 6 of the polygon with the vertical lines A and B shown below, the resulting figure forms the two-strand string S shown below at the right.

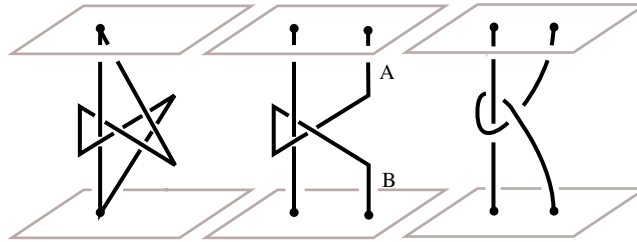


Figure 14: Correspondance between polygons and strings.

As long as vertex 3 is below vertex 6, there is no obstacle to drawing A and B . Further, the edge lengths specified above prevent edges 3, 4, and 5 from crossing either of the planes shown above.

Thus, the portion of the polygon between these two planes always corresponds to the same two-strand string as long as vertex 3 is below vertex 6. First, we will study the string S in the continuous category. Then we will prove that the polygon always corresponds to the same string, i.e. that it cannot be deformed (while preserving geometry and string type), to make vertices 3 and 6 have the same z coordinate.

As a first step, let's look at the string S in the continuous category.

Lemma 8. *The two-strand string S is nontrivial.*

Proof. It is a simple observation that if a two-strand string is trivial, connecting the two strands on top and on the bottom must give an unknot. After all, a string-isotopy to the trivial string can easily be promoted to a knot-isotopy of the corresponding knot to the unknot.

On the other hand, connecting the strands of our string in this fashion yields the trefoil. \square

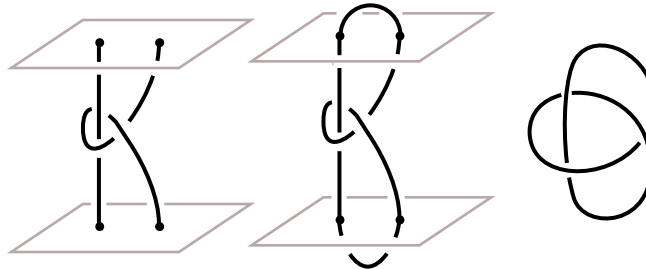


Figure 15: Connecting the ends gives the trefoil.

The theory of strings now tells us that the right strand must always encircle the left.

Lemma 9. *Any nontrivial two-strand string, such that the first strand is a straight line, and the second strand is unknotted, has the property that the second strand encircles the line.*

Proof. To see this, suppose that the second strand does not encircle the line. Taking a top view, as below, we see that the line can be moved away from the other strand.

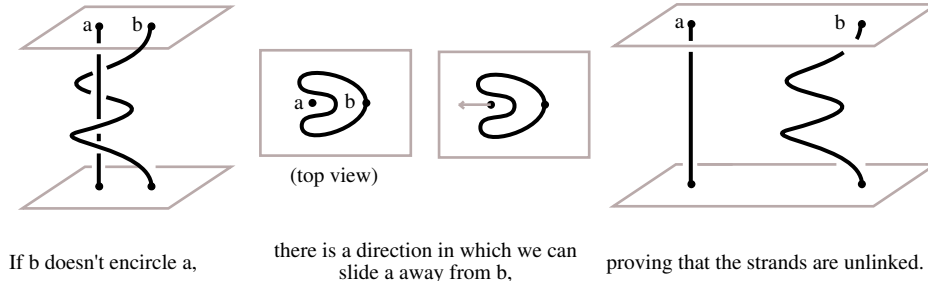


Figure 16: One strand must encircle the other.

Since the second strand is itself unknotted, we can isotope it into another straight line, proving that the string is trivial. \square

Since the right strand is composed of just three sticks, the fact that it encircles edge 1 means that vertices 3 and 6 can each be no more than $l_3 + l_4$ units from edge 1. But for the two to share a horizontal plane, their combined distance from edge 1 must be substantially greater.

To see this, observe that the diagram below captures the situation when vertices 3 and 6 share a horizontal plane at height e above vertex 1. For simplicity the diagram omits the second strand, (edges 3, 4, and 5), and includes only edges 1, 2, and 6. We also rescale so that the first edge has length one. The diagram shows edges 2 and 6 rotated into the same plane and adds a line (of length d) through vertices 3 and 6 perpendicular to edge 1. We now show that we can push either vertex 3 or vertex 6 close to the z -axis, but not both at once.

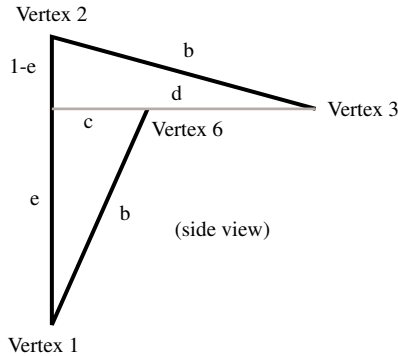


Figure 17: Geometry of vertices 3 and 6.

From the diagram, we have $d^2 + (1 - e)^2 = b^2$, and $c^2 + e^2 = b^2$. Thus we have $c^2 + d^2 = 2b^2 + 2e(1 - e) - 1$. Now $2e(1 - e)$ is least when e is least, and clearly $e > 1 - b$, so we have $c^2 + d^2 > 2b - 1$.

Returning to our original notation for edge lengths, $(c/l_1)^2 + (d/l_1)^2 > 2(l_2/l_1) - 1$. We proved above that c and d are each less than $l_3 + l_4$. Thus, if the l_i satisfy $(l_3 + l_4)^2 < l_1 l_2 - (l_1)^2/2$, our polygon cannot be isotoped so that 3 and 6 share a horizontal plane. The edge lengths of the example above satisfy this condition.

This means that any polygon-isotopy corresponds to a string-isotopy of the central string, and hence must preserve string type. Since this string type is nontrivial by our lemma above, no polygon-isotopy can deform our polygon to the standard unknotted polygon. \square

We remark that this result can easily be extended to Pol_n . To extend the result to Pol_n , add more corners (but not more length!) to the fourth edge, as below. The above proof goes through again, with the minor change that we use vertex 3 and vertex n , and each cannot move farther away from the z -axis than the distance $l_3 + l_4 + \dots + l_{n-3}$. The resulting knot looks like this:

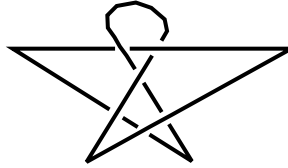


Figure 18: An example in Pol_n .

Of course, we could as easily have tied a small knot in this section, or attached a small link, without changing the situation. Thus, stuck examples exist in every knot and link type.

To see that there are many types of unknots for large n , realize that with enough joints, we could replace the string S with the connected sum $S\#S$. This is a different string type from S (connecting the ends as in Lemma 8 gives the connected sum of two trefoils), which corresponds to an unknotted polygon, so there are three types of unknots in Pol_n for some n .

With enough vertices, we can take the connected sum any finite number of times, creating an arbitrarily large family of different stuck unknots.

We have proved:

Corollary 1. *For suitable choices of edge length, there are multiple classes of unknots in Pol_n for any $n > 5$. For any knot or link type, there exists some n in which there are geometrically different examples of that knot or link type. The number of different embedding classes of a given knot type increases with n , becoming arbitrarily large as $n \rightarrow \infty$.*

4. Conclusion and Further Directions

It would be interesting to extend the results here to a complete classification of the connected components of Pol_6 for any edge lengths. This seems to be a hard problem. We suspect that all stuck unknots in Pol_6 resemble the example above. However, the algebraic condition for the edge lengths given in the proof of Theorem 2 is certainly not sharp! The proof above contains too many simplifications for the converse to follow easily.

It would also be interesting to obtain bounds on the number of classes of unknots in Pol_n as a function of n . In this direction, bounds on the number of connected components of Pol_n derived from examining the homology of the set of singular polygons could be combined with existing bounds on the number of knots with stick number n to deduce the existence of “extra” embedding classes derived from geometry rather than topology. We conjecture that the number of embedding classes of the unknot grows geometrically in n .

Acknowledgements

The authors would like to thank Jon Simon for introducing them to this problem, and Elizabeth Dowling for her gracious hospitality during the preparation of this paper.

References

- [1] R. Randell, *A molecular conformation space*, *MATH/CHEM/COMP 1987*, Studies in Physical and Theoretical Chemistry **54** (1988), 125-140.
- [2] K. Millett, *Knottting of regular polygons in 3-space*, *J. Knot Theory Ramifications* **3** (1994), 263-278.
- [3] J. Simon, *Energy functions for polygonal knots*, *J. Knot Theory Ramifications* **3** (1994), 299-320.
- [4] Y. Diao, C. Ernst, E.J. Janse van Rensburg, *In search of a good polygonal knot energy*, *J. Knot Theory Ramifications* **6** (1997), 633-658.
- [5] D.W. Sumners and S.G. Whittington, *Knots in self-avoiding walks*, *J. Phys. A: Math. Gen.* **21** (1988), 1689-1694.
- [6] J.A. Calvo, *The embedding space of hexagonal knots*, preprint, (1998).